Atmos. Chem. Phys., 24, 11911–11925, 2024
https://doi.org/10.5194/acp-24-11911-2024

Atmospheric Chemistry and Physics
Open Access
EGU

Research article

Changing optical properties of black carbon and brown carbon aerosols during long-range transport from the Indo-Gangetic Plain to the equatorial Indian Ocean

Krishnakant Budhavant[1,4], Mohanan Remani Manoj[2], Hari Ram Chandrika Rajendran Nair[2], Samuel Mwaniki Gaita[2], Henry Holmstrand[2], Abdus Salam[3], Ahmed Muslim[1], Sreedharan Krishnakumari Satheesh[4], and Örjan Gustafsson[2]

[1]Maldives Climate Observatory at Hanimaadhoo, Maldives Meteorological Service, Hanimaadhoo, 02020, Maldives
[2]Department of Environmental Science and the Bolin Centre for Climate Research, Stockholm University, 10691 Stockholm, Sweden
[3]Department of Chemistry, University of Dhaka, Dhaka 1000, Bangladesh
[4]Divecha Centre for Climate Change, Indian Institute of Science, Bangalore 560012, India

Correspondence: Örjan Gustafsson (orjan.gustafsson@aces.su.se)

Received: 12 January 2024 – Discussion started: 17 January 2024
Revised: 20 April 2024 – Accepted: 18 August 2024 – Published: 24 October 2024

Abstract. Atmospheric aerosols strongly influence the global climate through their light absorption properties (e.g., black carbon (BC) and brown carbon (BrC)) and scattering properties (e.g., sulfate). This study presents simultaneous measurements of ambient-aerosol light absorption properties and chemical composition obtained at three large-footprint southern Asian receptor sites during the South Asian Pollution Experiment (SAPOEX) from December 2017 to March 2018. The BC mass absorption cross section (BC-MAC_{678}) values increased from 3.5 ± 1.3 at the Bangladesh Climate Observatory at Bhola (BCOB), located at the exit outflow of the Indo-Gangetic Plain, to 6.4 ± 1.3 at two regional receptor observatories, the Maldives Climate Observatory at Hanimaadhoo (MCOH) and the Maldives Climate Observatory at Gan (MCOG), representing an increase of 80 %. This likely reflects a scavenging fractionation, resulting in a population of finer BC with higher MAC_{678} that has greater longevity. At the same time, BrC-MAC_{365} decreased by a factor of 3 from the Indo-Gangetic Plain (IGP) exit to the equatorial Indian Ocean, likely due to photochemical bleaching of organic chromophores. The high chlorine-to-sodium ratio at the BCOB, located near the source region, suggests a significant contribution of chorine from anthropogenic activities. Particulate Cl^- has the potential to be converted into Cl radicals, which can affect the oxidation capacity of polluted air. Moreover, Cl^- is shown to be nearly fully consumed during long-range transport. The results of this synoptic study, conducted on a large southern Asian scale, provide rare observational constraints on the optical properties of ambient BC (and BrC) aerosols over regional scales, away from emission sources. They also contribute significantly to understanding the aging effect of the optical and chemical properties of aerosols as pollution from the Indo-Gangetic Plain disperses over the tropical ocean.

Published by Copernicus Publications on behalf of the European Geosciences Union.

1 Introduction

Light-absorbing carbonaceous moieties represent a key component of atmospheric aerosols as they affect the global climate through both their direct absorption and combined/indirect effects with other components (Ramanathan and Carmichael, 2008; IPCC, 2021). The systematic underestimation of the total optical absorption of aerosols by a factor of 2 to 3 in climate models, compared to observation-based estimates, illustrates significant current uncertainties and potential systematic bias (Gustafsson and Ramanathan, 2016). In addition to climate effects, anthropogenic aerosols, such as black carbon (BC) and sulfate (SO_4^{2-}), can penetrate deeply into human lungs and increase the risk of cardiovascular and respiratory diseases (Mauderly and Chow, 2008; Lelieveld et al., 2015; WHO, 2016).

The aerosol loadings in the southern Asian region are much higher than the global average, primarily due to anthropogenic activities. The high levels of anthropogenic aerosols exert a strong influence on both the climate and the quality of the air people breathe in southern Asia, primarily due to massive emissions from the Indo-Gangetic Plain (IGP), a densely populated and industrialized part of northern India and Bangladesh (Shindell et al., 2012; Nair et al., 2023). These anthropogenic aerosols cause "regional dimming", which reduces the amount of sunlight that reaches the Earth's surface (Ramanathan et al., 2007; Nair et al., 2023). This, in turn, leads to decreased evaporation and rainfall, which can significantly impact agriculture and water resources (Bollasina et al., 2011). Furthermore, these aerosols have been linked to weakened monsoons responsible for most of the region's rainfall (Ramanathan et al., 2007). Additionally, these aerosols can intensify tropical storms, making them more destructive (Lin et al., 2023). Perhaps what is most concerning is that anthropogenic carbonaceous aerosols have been linked to the melting of the Himalayan glaciers (Ramanathan et al., 2007; Ramachandran et al., 2023). This is especially significant because the Himalayan watershed serves over 3 billion people, making it one of the most important water sources in the world.

BC and organic carbon (OC) aerosols are mainly emitted from incomplete fossil fuel combustion and biomass burning (Chakrabarty et al., 2016; Höpner et al., 2016; Dasari et al., 2019). Light-absorbing organic carbon, also known as brown carbon (BrC), consists of water-soluble and water-insoluble components. It is often categorized into water-soluble and methanol-soluble/water-insoluble BrC to describe its optical properties. BrC is predominantly produced by burning fossil fuels and biomass. It can also be generated via other methods, such as through the low-temperature oxidation of biogenic substances, the polymerization of its by-products, reactions involving dienes, and the atmospheric processing of anthropogenic or biogenic volatile organic compounds (VOCs) in the presence of NO_x (Andreae and Gelencsér, 2006; Laskin et al., 2015).

As per the current understanding, BC displays comparatively low reactivity and undergoes negligible changes over long distances. In contrast, BrC seems to be subject to bleaching (Dasari et al., 2019). It is, therefore, imperative to delve into the dynamics of the optical properties of BrC that are exhibited during its long-distance transportation. Accurate mass absorption cross section (MAC) measurements and the source apportionment of BC aerosols are also crucial as they serve as inputs for climate and air quality models (Ram and Sarin, 2009; Gustafsson and Ramanathan, 2016; Venkataraman et al., 2020). BC aerosols from fossil combustion have different light absorption/radiative effects and atmospheric fates compared to those from biomass combustion (Gustafsson and Ramanathan, 2016; Dasari et al., 2019; Budhavant et al., 2015, 2023). The emissions, source apportionment, and optical properties of anthropogenic aerosols from India and greater southern Asia represent a key uncertainty in climate and environmental research that urgently needs to be addressed.

Access to three strategically located atmospheric observatories in southern Asia provides an opportunity for synoptic observations of aerosols along the main wintertime flow trajectory, from the key source region for anthropogenic aerosols to the dispersal of these aerosols over regional scales in the northern Indian Ocean (Fig. 1). The arrows in Fig. 1 illustrate the common pathway of the well-pronounced South Asian winter monsoon outflow, projected from meteorological back-trajectory analyses. During the dry winter season, characterized by the highest loads of anthropogenic aerosols (e.g., BC, OC, non-sea-salt SO_4^{2-} (nss-SO_4^{2-}), and non-sea-salt K^+ (nss-K^+)), the Himalayas induce topographical steering that forces northern Indian air pollution into the northern Bay of Bengal (Fig. 1). The main flow then shifts southward, with many air parcels arriving at the Maldives Climate Observatory at Hanimaadhoo (MCOH) and the Maldives Climate Observatory at Gan (MCOG).

The South Asian Pollution Experiment 2018 (SAPOEX-18) was a large international campaign aimed at studying BC and BrC absorption properties during long-range transport in the southern Asian source receptor system using multiple approaches and sites. The current study reports on the ambient evolution of light-absorption properties for both BC and BrC (in connection with the chemical composition of aerosols) by combining in situ filter measurements, online optical-instrument data on the physical and chemical properties of aerosols, and satellite and remote sensing data sets. Observations were collected from three strategically located regional receptor sites. The Bangladesh Climate Observatory at Bhola (BCOB) intercepts the integrated outflow of the IGP in rural southern Bangladesh, along the shores of the Bay of Bengal. The MCOH, located in a northern atoll in the Maldives, and the MCOG, situated close to the Equator in the southernmost Maldivian atoll, are ideal locations for intercepting the larger footprint of the southern Asian outflow. Synoptic studies between the BCOB and the Indian Ocean

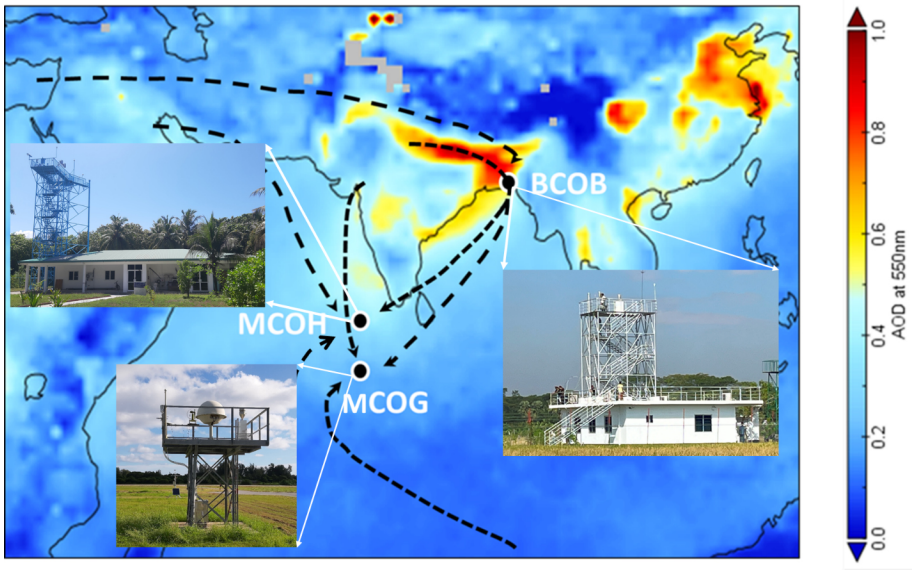

Figure 1. Average aerosol optical depth (AOD) at 550 nm obtained by the Moderate Resolution Imaging Spectroradiometer (MODIS) during the South Asian Pollution Experiment 2018 (SAPOEX-18) from December 2017 to March 2018 over the southern Asian region. The following receptor sites are shown (solid black circles accompanied by pictures): the Bangladesh Climate Observatory at Bhola (BCOB), the Maldives Climate Observatory at Hanimaadhoo (MCOH), and the Maldives Climate Observatory at Gan (MCOG). The thick black lines with arrows show the mean air mass trajectory clusters (more details are given in Figs. S1 and S4 in the Supplement).

receptor sites may shed light on the changing aerosol composition and optical/radiative effects that occur during long-range over-ocean transport. Finally, the observational constraints on aerosol composition and optical properties are crucial inputs for more accurate modeling of the radiative effects in this large region.

2 Methods

2.1 Aerosol sample collection

The work presented here was conducted at three sites – the BCOB (22.17° N, 90.71° E), the MCOH (6.78° N, 73.18° E), and the MCOG (0.69° S, 73.15° E) – from early December 2017 to the end of March 2021. The BCOB is located on Bhola Island (also called Dakhin Shāhbāzpur Island) in the delta of the Bay of Bengal, about 300 km south of Dhaka, Bangladesh (Ahmed et al., 2018; Shohel et al., 2018; Dasari et al., 2019). The MCOH is located in the northern part of the island of Hanimaadhoo (Thiladhunmathi Atoll), which covers around 3.1 km^2 and has around 1800 inhabitants (Corrigan et al., 2006; Höpner et al., 2016; Budhavant et al., 2023). Measurements are taken from a tower platform at 15 m above sea level, from which air samples are directed to a ground-level, air-conditioned laboratory (Corrigan et al., 2006; Budhavant et al., 2018, 2023). The MCOG is located on the southernmost island of the Maldives, at the Equator, 500 km south of the capital city (Malé) and 800 km from the MCOH (Corrigan et al., 2006; Ramanathan et al., 2007). Detailed descriptions of these observatories are available in earlier publications (Corrigan et al., 2006; Stone et al., 2007; Dasari et al., 2019). Aerosol $PM_{2.5}$ samples were collected using 150 mm diameter quartz filters pre-combusted at 450 °C (Merck Millipore), employing high-volume samplers (DH-77, Digitel Elektronik AG) at 500 L min^{-1}. Blank filters were shipped, stored, and processed identically to the samples. Each of these three observatories was instrumented to record spectral data on aerosol optical depth (AOD) as part of the AErosol RObotic NETwork (AERONET) (Holben et al., 1998; Ramanathan et al., 2005; Nair et al., 2023).

2.2 Chemical analysis of aerosol filter samples

The aerosols were analyzed for several carbonaceous components and major ions using standard protocols and suitable techniques (Dasari et al., 2019; Budhavant et al., 2023). The mass concentrations of elemental carbon (EC; here referred to as BC), OC, and total carbon (TC = BC + OC) were measured with a thermal–optical transmission analyzer (the Lab OC-EC Aerosol Analyzer from Sunset Laboratory) using the NIOSH 5040 method from the National Institute for Occupational Safety and Health (Birch and Cary, 1996; Budhavant et al., 2015, 2023). NIST-traceable laboratory standards (Reference Material 8785) were used to verify the accuracy of the OC, EC, and TC measurements. No detectable signal was observed for BC in field blanks. The OC concentration values were blank-corrected by subtracting an average field blank (5 % of sample signals). Following the established protocol,

water-soluble organic carbon (WSOC) was measured using a Shimadzu TOC-VCPH analyzer (Kirillova et al., 2010, 2013; Budhavant et al., 2020).

Another portion of each aerosol filter was extracted with 18 MΩ cm Milli-Q water for the analysis of water-soluble inorganic ions using a Dionex Aquion ion chromatography (IC) system (Thermo Scientific). The system contains a guard column and an anion–cation separator column with a primary exchange resign and suppressor column (AERS 500/CERS 500). The quality of the data was tested with internal and external reference samples. The analytical error was less than 4 % for the anions and 5 % for the cations. A more detailed description can be found in Budhavant et al. (2023).

2.3 Aerosol absorption measurements

The relationship between atmospheric concentration and direct radiative forcing by BC is characterized by its mass absorption cross section (MAC). The laser beam (678 nm) of the Sunset Laboratory aerosol carbon analyzer was used to measure the light attenuation ($\mathrm{ATN} = -\ln(I/I_0)$) of the aerosols on the filter (Ram and Sarin, 2009). The MAC for BC ($\mathrm{MAC_{BC}}$) is calculated as follows (Weingartner et al., 2003; Budhavant et al., 2020):

$$\mathrm{MAC_{BC}} = \frac{\mathrm{ATN}}{\mathrm{BC_{loading}} \cdot \mathrm{MS} \cdot R(\mathrm{ATN})}, \quad (1)$$

where MS is an empirical multiple-scattering correction factor implemented in most filter-loading correction schemes. To account for the multiple-scattering effects, a factor of 4.5 was selected for estimation (Budhavant et al., 2020). Correction for non-linearity when measuring light absorption through a filter is denoted by R.

$$R = \left(\frac{1}{1.114} - 1\right)\left(\frac{\ln(\mathrm{ATN}) - \ln(0.1)}{\ln(0.5) - \ln(0.1)}\right) + 1 \quad (2)$$

The spectrophotometer measured the light absorption of the aerosol extracted from water. Subsequently, the MAC was calculated for water-soluble BrC (WS-BrC).

$$\mathrm{MAC_{WS\text{-}BrC}} = \frac{b_{\mathrm{abs},365}}{[\mathrm{WSOC}]}, \quad (3)$$

where WSOC is the water-soluble organic carbon concentration and $b_{\mathrm{abs},365}$ is the absorption coefficient at 365 nm. The absorption Ångström exponent (AAE) was estimated as the slope in a linear regression of the logarithm of the absorption coefficient (b_{abs}) versus the logarithm of the wavelength (λ).

$$\ln|b_{\mathrm{abs}}(\lambda)| = -\mathrm{AAE} \cdot \ln|\lambda| + \mathrm{intercept} \quad (4)$$

The AAE was fitted between 330–400 nm to avoid interference from other light-absorbing solutes, such as ammonium nitrate, sodium nitrate, and nitrate ions (Cheng et al., 2011; Bosch et al., 2014).

2.4 Aerosol radiative forcing

The radiative forcing of aerosol particles is a major uncertainty factor in understanding the Earth's climate (Ramanathan et al., 2007; IPCC, 2021; Lu et al., 2023). The radiative implications of aerosols are quantified in terms of their direct aerosol radiative effects (DAREs). Spectral aerosol-optical-depth (AOD) data from three stations associated with the AErosol RObotic NETwork (AERONET) (Hess et al., 1998; Bedareva et al., 2014), ozone data from the Ozone Monitoring Instrument (OMI), water vapor and surface reflectance data from the Moderate Resolution Imaging Spectroradiometer (MODIS), and further surface reflectance data were used in this study. The aerosol optical model (version 3.1 of OPAC (Optical Properties of Aerosols and Clouds)), which works based on Mie scattering theory (Hess et al., 1998), was used to estimate the optical properties of newly defined aerosol mixtures (Hess et al., 1998). AOD measurements from sun photometers, single scattering albedo (SSA), and asymmetry parameters modeled using the Mie scattering model were used as inputs for the Santa Barbara DISORT Atmospheric Radiative Transfer (SBDART) model (Ricchiazzi et al., 1998; Lu et al., 2023). This model uses a complex discrete-ordinate method to numerically integrate the radiative-transfer equations (Stamnes et al., 1988). A detailed description of this model and approach is available elsewhere (Ramanathan et al., 2005; Satheesh, 2002; Nair et al., 2023).

2.5 Air mass back trajectories and remote sensing

This study examines air mass back trajectories to identify potential sources of BC and other aerosol components arriving at the MCOG station, which is even further away from the source regions than the MCOH. Given the long-distance travel involved, the focus on the dry season (increasing longevity), the understanding that BC has a longer lifetime than other aerosols, and the experiences from earlier studies (Budhavant et al., 2020, 2023), a back-trajectory (BT) time horizon of 10 days was selected as appropriate. The air mass back trajectories (AMBTs) were generated at an arrival height of 50m at all three sampling sites (Figs. S1–S4 in the Supplement) using the NOAA Hybrid Single-Particle Lagrangian Integrated Trajectory model (version 4) (Draxler and Hess, 1997; Draxler, 1999). This study's calculations were based on meteorological data from the Global Data Assimilation System (GDAS), which is run four times daily (at 00:00, 06:00, 12:00, and 18:00 UTC). These individual trajectories were clustered into different geographical regions (Fig. 1). The MODIS (Moderate Resolution Imaging Spectroradiometer) satellite-derived FIRMS (Fire Information for Resource Management System) fire-count data were combined with cluster analysis to understand the impact of biomass-burning emissions from potential source regions observed during the sampling period (Fig. 1).

3 Results and discussion

3.1 Atmospheric transport

The AMBTs, AOD measurements, and active fire data were used as parameters to study atmospheric transport and geographical source regions in the area. Based on atmospheric transport, we defined two temporal source domains: the influence of the heavily polluted Indo-Gangetic Plain (IGP) region (from 18 December 2017 to 8 February 2018) and the total period of the study. Measurements obtained at the BCOB represent an accumulation of IGP sources through air mass transport across northern Pakistan, northern India, and Bangladesh – a region containing many large cities and megacities, areas of heavy industrialization, and rural areas with extensive agricultural burning (Figs. 1 and S2). The MCOH and the MCOG are situated in the northern Indian Ocean and thus intercept long-range pollutant emissions from southern Asia, including the IGP, the western part of India, and the Indian Ocean (Figs. S3 and S4). Occasionally, winds in the IGP sector come from southern India or the Bay of Bengal. However, during winter, polluted winds from the IGP can reach the Bay of Bengal, leading to similar signals being detected over the MCOH and MCOG regions. This is particularly noticeable during synoptic observations. Cluster analysis of AMBTs, combined with AOD data, satellite measurements, and aerosol chemical composition, demonstrated that the wintertime northern Indian Ocean is greatly influenced by anthropogenic aerosols transported from source regions like the IGP and the western margin of India.

3.2 Organic carbon and black carbon

In general, varying primary and secondary sources, combined with the short atmospheric residence times of aerosol particles containing a high fraction of organic carbon, result in large regional differences in chemical composition, morphology, mixing state, size, and optical properties. OC was the main component of carbonaceous aerosols during the southern Asian winter, accounting for 85 ± 5 % of total carbon (TC) at the BCOB, 66 ± 9 % at the MCOH, and 67 ± 9 % at the MCOG. The OC contribution to TC was highest when the wind came from the IGP (Fig. 2) and lowest when the wind traveled over oceanic regions at all three sites. BC and OC are very well correlated ($R > 0.74$) at all three sampling sites, indicating similar source emissions. However, the average ratio of OC to BC was 6.5 ± 2.1 at the BCOB, decreasing markedly to 2.2 ± 1.1 at the MCOH and 2.4 ± 1.8 at the MCOG. This large decrease from the exit of the IGP source region (BCOB) to the Indian Ocean receptor sites (MCOH and MCOG) demonstrates that OC/BC ratios were strongly affected by selective processing and/or washout of OC during long-range transport (LRT). The atmospheric lifetime of OC is typically shorter than that of BC in this region (Budhavant et al., 2020). Since OC represents a more complex mixture, it is subject to more atmospheric transformation than BC, as reflected in the comparatively large shift in the stable-isotope fingerprints of the OC component from the source to the receptor sites in this region (Dasari et al., 2019; Bosch et al., 2014; Kirillova et al., 2016). The highest concentrations of BC, OC, and nss-SO_4^{2-} aerosols were associated with air masses from the IGP and the western margin of India.

The water-insoluble fraction of BrC exhibits a higher absorption rate per unit mass than the WS fraction (Liu et al., 2013; Cheng et al., 2016). We observed that the WSOC comprised a large but declining proportion of the overall OC (Fig. 3). The WSOC/OC ratio changed throughout the study, as shown in Fig. 4c. At the BCOB, the WSOC/OC ratio (0.35 ± 0.06) was less variable, indicating that the sources of both types of carbon were similar. Furthermore, we discovered a strong correlation between WSOC and OC concentrations at the BCOB ($r = 0.95$; $p < 0.001$). However, the lower WSOC/OC ratios at the MCOH (0.21 ± 0.1) and the BCOB (0.16 ± 0.1) suggest a higher contribution of water-insoluble OC at these locations and times. Carbonaceous aerosols derived from fossil fuel combustion may be less water-soluble (WSOC ≥ 20 %) due to the presence of fewer oxygenated organic moieties (Ruellan and Cachier, 2001). The mass fraction of WSOC relative to OC was observed as an indicator of aerosol photochemical processing in the atmosphere (Dasari et al., 2019). Overall, the decreasing OC/BC ratio from the IGP exit to after transportation over the ocean indicates that selective washout and bleaching reactions of organic carbon occurred.

3.3 Characteristics of the ionic aerosol components

The chemical composition of the aerosols changed both between sites and over time (Table 1; Fig. 2). Filter samples were characterized in terms of major anions (Cl^-, NO_3^-, and SO_4^{2-}) and major cations (Na^+, K^+, Mg^{2+}, Ca^{2+}, and NH_4^+) for the 4-month sampling period (Fig. 4). The highest concentrations of ions were recorded at the BCOB, which is expected as this site is situated at the outflow of the highly polluted IGP. However, the concentrations of SO_4^{2-} and NH_4^+ followed a different pattern. Higher values for SO_4^{2-} and NH_4^+ were observed at the MCOH. These MCOH-intercepted pollutants were traced to India's central and eastern regions and the IGP through AMBTs. The IGP region and its surrounding areas are hotspots for sulfur dioxide (SO_2) emissions, mainly due to the presence of multiple thermal power plants, construction industries, and petroleum refineries. These sources contribute to the region's SO_2 and nitrogen oxide (NO_x) levels (Guttikunda and Jawahar, 2014; Kuttippurath et al., 2022). Furthermore, a previous study conducted at the MCOH found that dimethyl sulfide (DMS) accounts for only up to 3 % of nss-SO_4^{2-} in polluted air (Granat et al., 2010). The IGP is a hotspot of high anthropogenic aerosol loading due to intense agricultural crop residue burn-

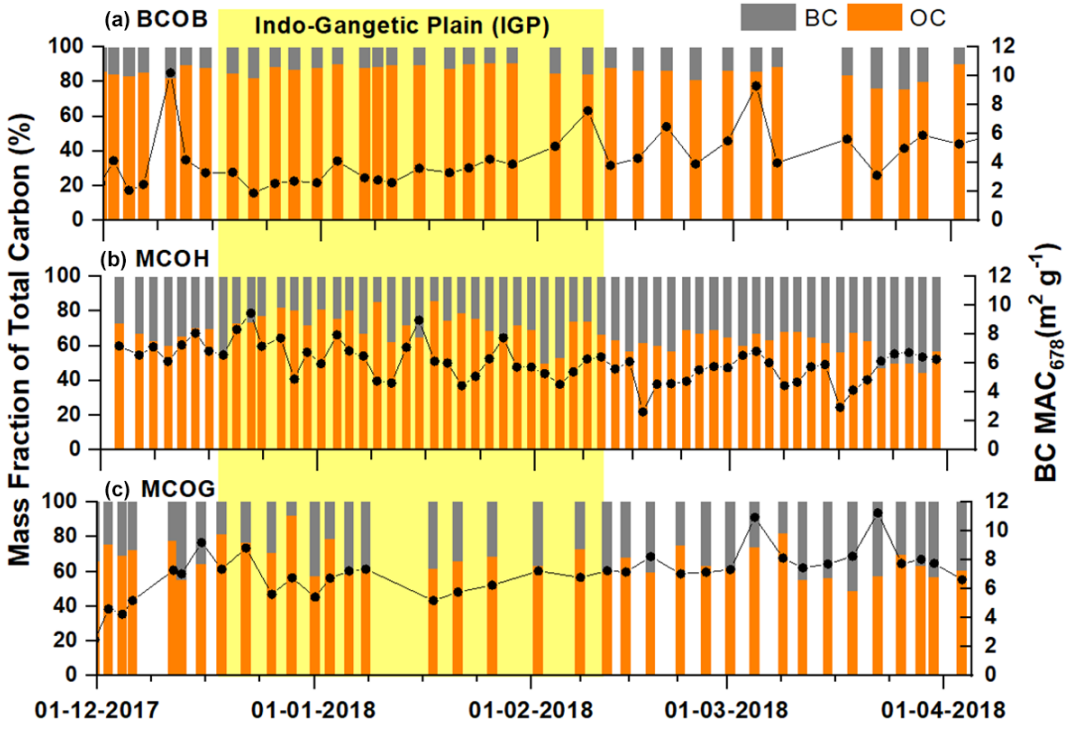

Figure 2. The mass fraction of total carbon (black carbon + organic carbon) and the BC mass absorption cross section (BC MAC) at 678 nm were measured at three receptor sites in southern Asia, i.e., at **(a)** the Bangladesh Climate Observatory at Bhola (BCOB), **(b)** the Maldives Climate Observatory at Hanimaadhoo (MCOH), and **(c)** the Maldives Climate Observatory at Gan (MCOG), from 1 December 2017 to early April 2018. The vertical yellow field indicates the predominance of air masses originating from the high-pollution source region of the Indo-Gangetic Plain (IGP).

ing, biomass burning, open waste burning, industrial activities, and high urbanization (Dasari et al., 2020; Ansari and Ramachandran, 2023; Nair et al., 2024).

To identify the effect of marine influences on aerosol composition, sea salt corrections were calculated using Na^+ as the reference element (Keene et al., 1986). The nss-SO_4^{2-} fraction relative to total sulfate was observed at the BCOB (99 ± 1 % (mean $\pm$ standard deviation)), the MCOH (98 ± 1 %), and the MCOG (86 ± 13 %), indicating significant contributions of SO_4^{2-} and SO_2 from diesel combustion and coal-fired power plants in India and Bangladesh. Some nss-SO_4^{2-} observed at the MCOH may have been due to ocean traffic over the northern Indian Ocean as the majority of shipping emissions result from fuel combustion that releases SO_x (sulfur oxide) and NO_x directly into the atmosphere (Corbett and Koehler, 2003; Gopikrishnan and Kuttippurath, 2021).

The BCOB, located near the IGP source region, was found to have a high Cl^-/Na^+ ratio (4.7 ± 3.5; Fig. 4) compared to the other two receptor sites (Fig. 4). This implies that, at the BCOB, a significant amount of total Cl^- comes from anthropogenic activities. The particulate Cl^- might come from the burning of plastics containing chlorine, such as polyvinyl chloride (PVC), during open waste burning (Pathak et al., 2023). This can lead to the formation of Cl^- radicals, which impact the oxidation capacity of polluted air. Marine aerosols often experience chlorine depletion, and releasing gas-phase HCl from particles can impact aerosol acidity and the concentration of water-soluble ions. However, once these particles enter the atmosphere, they become exposed to various pollutants, leading to the loss of particulate chlorine as it transitions into the gaseous phase. This loss of chlorine is typically attributed to ion exchange reactions with atmospheric acids like SO_2, H_2SO_4, and HNO_3, which result in the formation of sulfates and nitrates, as well as the degassing of HCl (Orsini et al., 1986; Brimblecombe and Clegg, 1988; Haslett et al., 2023). Other pathways lead to the loss of particulate chlorine, such as interactions with NO, N_2O_5, HOBr, and O_3, as well as the release of NOCl, HONO, $ClNO_2$, Cl_2, and BrC (Vogt et al., 1996; Behnke and Zetzsch, 1989; Haslett et al., 2023). These pathways can have significant implications for marine tropospheric chemistry and the polluted coastal atmosphere due to the creation of photochemically active, halogenated gaseous compounds. This study found significant anthropogenic chloride emissions from human activities, which can affect the oxidation capacity of polluted air.

We observed a high correlation ($r \geq 0.7$) between BC, OC, and nss-K^+ in aerosol samples collected at the BCOB (Table S1 in the Supplement) and the MCOH (Table S2).

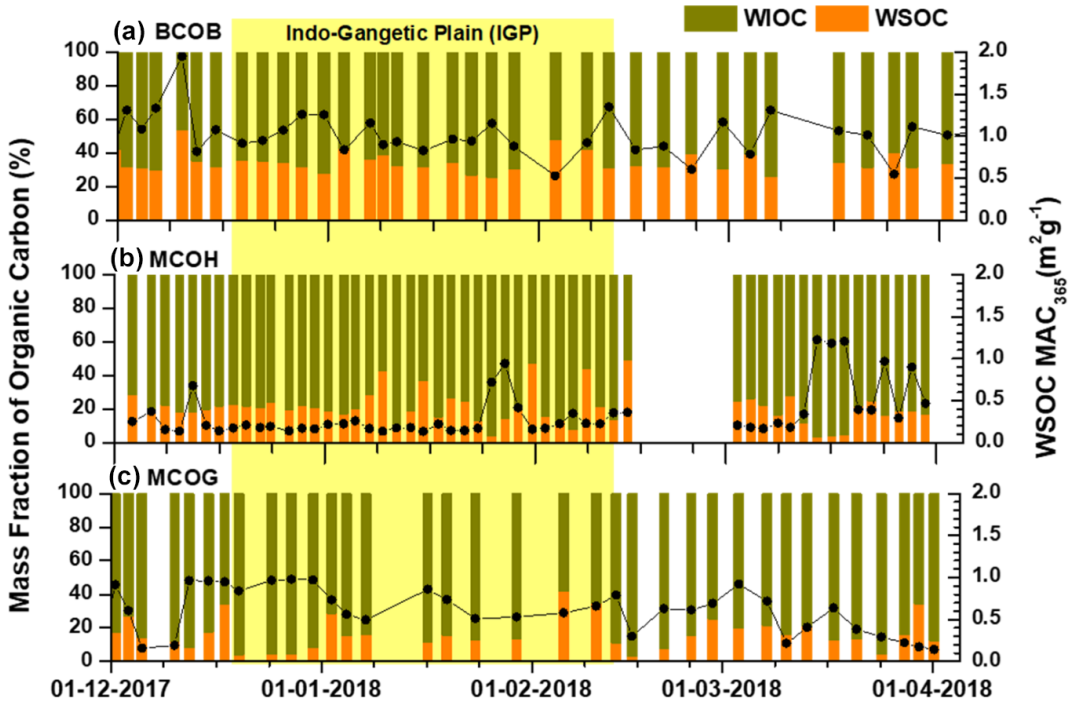

Figure 3. The mass fraction of organic carbon (divided into water-insoluble organic carbon (WIOC) and water-soluble organic carbon) and the mass absorption cross section for brown carbon (BrC MAC) at 365 nm (MAC_{365}) were measured at three receptor sites in southern Asia, i.e., at **(a)** the Bangladesh Climate Observatory at Bhola (BCOB), **(b)** the Maldives Climate Observatory at Hanimaadhoo (MCOH), and **(c)** the Maldives Climate Observatory at Gan (MCOG), from 1 December 2017 to early April 2018. The vertical yellow field indicates the predominance of air masses originating from the high-pollution source region of the Indo-Gangetic Plain (IGP).

Table 1. Aerosol optical depth (AOD); the mass absorption cross sections (MACs) of black carbon (BC) and brown carbon (BrC); the concentrations of BC, organic carbon (OC), and water-soluble organic carbon (WSOC); and the absorption Ångström exponent (AAE) were measured at the Bangladesh Climate Observatory at Bhola (BCOB), the Maldives Climate Observatory at Hanimaadhoo (MCOH), and the Maldives Climate Observatory at Gan (MCOG) from November 2017 to March 2018. BC-MAC_{678} refers to the BC MAC at 678 nm, while BrC-MAC_{365} refers to the BrC MAC at 365 nm.

Site	AOD	BC-MAC_{678} ($m^2\,g^{-1}$)	BrC-MAC_{365} ($m^2\,g^{-1}$)	BC ($\mu g\,m^{-3}$)	OC ($\mu g\,m^{-3}$)	WSOC ($\mu g\,m^{-3}$)	AAE_{BrC} (330–400 nm)
BCOB	0.8 ± 0.3	4.4 ± 1.9	1.0 ± 0.3	3.0 ± 1.3	20 ± 11	6.9 ± 4.0	5.5 ± 2.7
MCOH	0.5 ± 0.2	6.1 ± 1.3	0.3 ± 0.3	1.0 ± 0.5	2.3 ± 1.5	0.5 ± 0.4	6.5 ± 2.4
MCOG	0.2 ± 0.1	7.0 ± 1.9	0.6 ± 0.3	0.3 ± 0.3	0.7 ± 0.5	0.1 ± 0.1	4.1 ± 0.5
Only during the synoptic period (18 December 2017 to 8 February 2018)							
BCOB	0.9 ± 0.4	3.5 ± 1.3	1.0 ± 0.2	3.6 ± 1.0	27 ± 8.7	9.1 ± 2.8	6.4 ± 2.0
MCOH	0.5 ± 0.2	6.4 ± 1.3	0.2 ± 2.0	1.1 ± 0.5	3.0 ± 1.6	0.6 ± 0.4	7.6 ± 1.5
MCOG	0.3 ± 0.2	6.4 ± 1.7	0.7 ± 0.2	0.5 ± 0.2	0.9 ± 0.4	0.1 ± 0.1	4.0 ± 0.9

The nss-K^+ fraction of total potassium was observed at the BCOB ($97 \pm 3\,\%$), the MCOH ($78 \pm 13\,\%$), and the MCOG ($42 \pm 33\,\%$), indicating significant contributions from biomass burning at the BCOB and MCOH as nss-K^+ is considered a proxy for identifying the regional impact of biomass-burning emissions (Andreae, 1983; Paris et al., 2010). High concentrations of nss-SO_4^{2-}, nss-K^+, and NH_4^+ in the measured ions and carbon aerosols indicate strong anthropogenic sources for the ambient aerosols over the northern Indian Ocean (Table 2).

Our observations show an increase in the SO_4^{2-}/BC ratio when aerosols are transported from the IGP. Notably, this ratio is more pronounced at the MCOH than at the BCOB (Fig. 5). This shift in composition likely signifies the generation of secondary sulfate from anthropogenic SO_2 during extended transportation. It was observed that there was

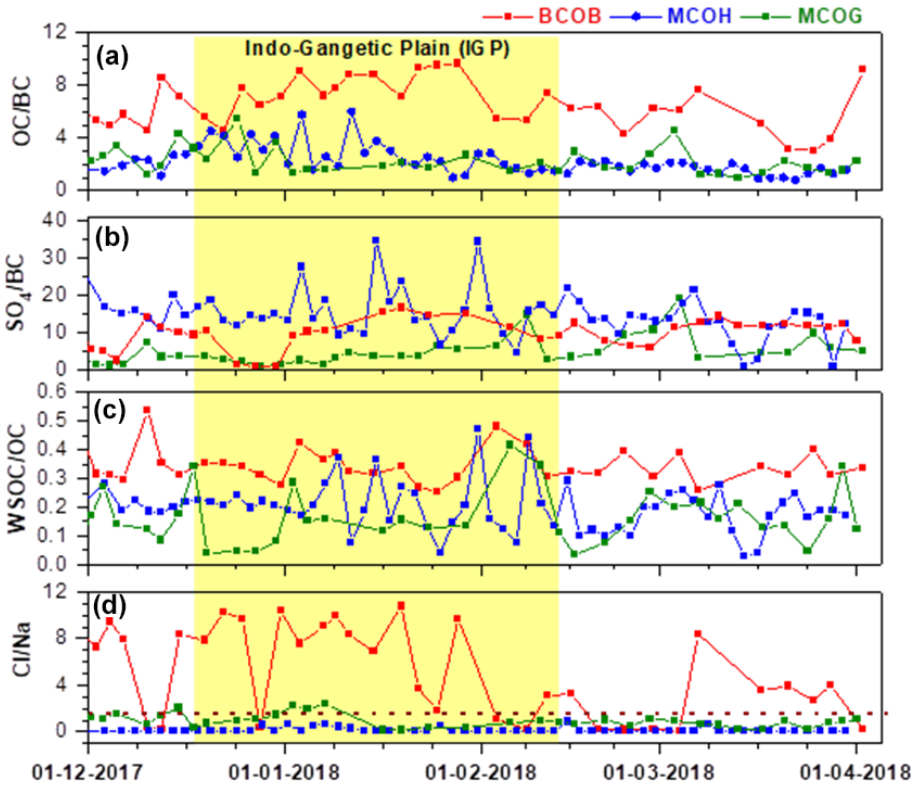

Figure 4. Time series of the ratios of the measured chemical species (OC/EC **(a)**, SO_4/BC **(b)**, WSOC/BC **(c)**, and Cl/Na **(d)**), with a seawater ratio of 1.8 (represented by the dotted line), over three receptor sites in southern Asia: the Bangladesh Climate Observatory at Bhola (BCOB), the Maldives Climate Observatory at Hanimaadhoo (MCOH), and the Maldives Climate Observatory at Gan (MCOG).

Table 2. Concentrations of major ions ($\mu g\,m^{-3}$) were measured at the Bangladesh Climate Observatory at Bhola (BCOB), the Maldives Climate Observatory at Hanimaadhoo (MCOH), and the Maldives Climate Observatory at Gan (MCOG) from November 2017 to March 2018.

Site	Na^+	Cl^-	NO_3^-	NH_4^+	nss-SO_4^{2-}	nss-K^+	Ca^{2+}
BCOB	0.4 ± 0.3	1.9 ± 1.8	7.6 ± 7.3	3.8 ± 3.2	11 ± 5	2.4 ± 1.2	0.1 ± 0.1
MCOH	0.8 ± 0.5	0.7 ± 0.5	0.1 ± 0.0	4.2 ± 2.7	11 ± 7	0.4 ± 0.3	0.1 ± 0.0
MCOG	1.0 ± 0.9	0.8 ± 0.8	0.3 ± 0.4	0.5 ± 0.8	3.0 ± 2	0.1 ± 0.1	0.2 ± 0.2
Only during the synoptic period (18 December 2017 to 8 February 2018)							
BCOB	0.5 ± 0.4	3.0 ± 1.9	12 ± 7.7	2.5 ± 3.5	12 ± 5	2.9 ± 1.0	0.1 ± 0.1
MCOH	1.0 ± 0.5	0.6 ± 0.4	0.1 ± 0.0	4.8 ± 3.6	16 ± 7	0.5 ± 0.3	0.1 ± 0.0
MCOG	1.1 ± 1.1	0.6 ± 0.4	0.3 ± 0.3	0.9 ± 0.1	4.7 ± 4	0.1 ± 0.1	0.2 ± 0.2

a lower SO_4^{2-}/BC ratio at the MCOG than at the MCOH. This might be because SO_4^{2-} is washed out more easily than BC in this region (Budhavant et al., 2020), and another factor is that the MCOG has slightly different AMBT paths than the MCOH (Fig. 1). It is worth noting that there may be some minor sources of emissions, such as ships and small islands, along the route to the receptor sites. However, their impact on the overall regional loading of BC is insignificant. Therefore, we can infer that most BC loading over the northern Indian Ocean originates from high-emission source areas in southern Asia. While there was an increase in the SO_4^{2-}/BC ratio, two other important coating components, the WSOC/BC and WIOC/BC ratios (where WIOC denotes water-insoluble organic carbon), declined.

3.4 Black carbon mass absorption cross section

The impact of BC aerosols on air quality, boundary layer dynamics, and climate depends not only on BC concentration but also on the light absorption characteristics of BC. Moreover, MAC values are crucial for estimating radiative forcing accurately. The MAC of BC is here denoted as "BC-

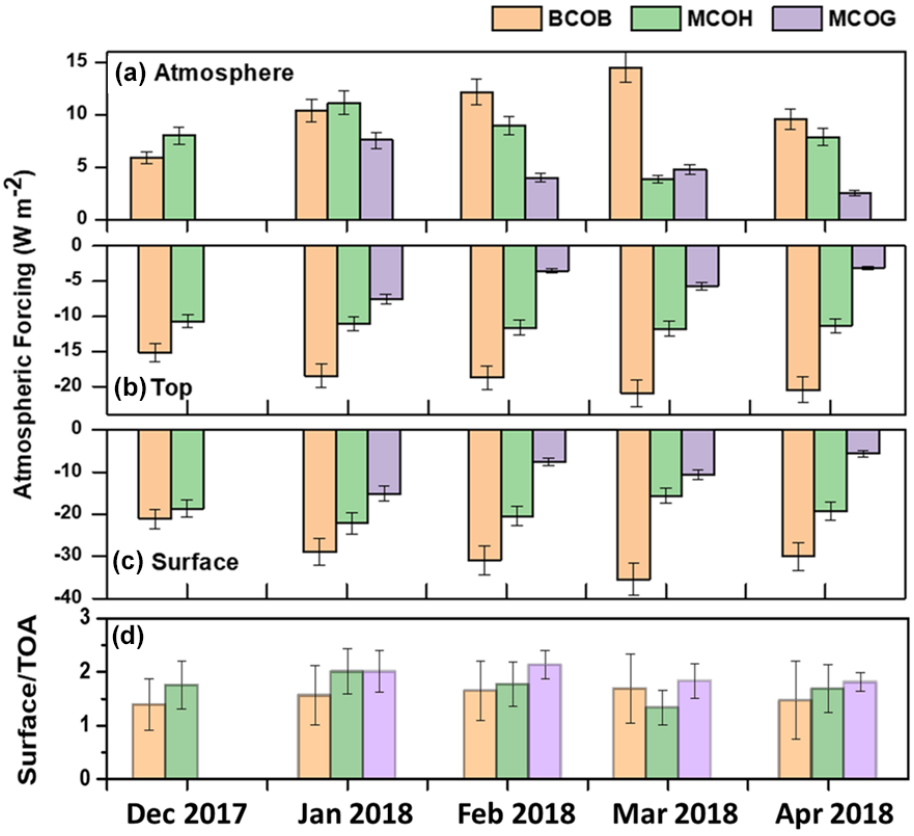

Figure 5. Monthly averaged direct aerosol radiative forcing (cloud-free atmosphere) was calculated for the locations of the Bangladesh Climate Observatory at Bhola (BCOB), the Maldives Climate Observatory at Hanimaadhoo (MCOH), and the Maldives Climate Observatory at Gan (MCOG) from December 2017 to April 2018. **(a)** Atmosphere forcing, **(b)** top-of-the-atmosphere (TOA) forcing, **(c)** surface forcing, and **(d)** the ratio of surface forcing to TOA forcing are shown.

MAC_{678}". During the SAPOEX-18 campaign, the calculated value of BC-MAC_{678} was found to have a lower average value at the BCOB ($4.4 \pm 1.9\,m^2\,g^{-1}$) and a higher average value at the most distant Indian Ocean receptor station, the MCOG ($7.0 \pm 1.9\,m^2\,g^{-1}$), with the MCOH, at a shorter over-ocean transport distance, having a value of $6.1 \pm 1.3\,m^2\,g^{-1}$ (Fig. 2). A recent laboratory-based study of the coating enhancement of the BC MAC (E-MAC) from these observatories showed that the E-MAC value was about 1.6 at all three stations (indicating a 60 % enhancement in the net BC MAC due to coating effects). This constancy suggests that the coating-aging effect of BC was nearly complete upon arrival at the BCOB (Nair et al., 2024). The approximately 80 % increase in BC-MAC_{678} during over-ocean transport must therefore signal another mechanism. It likely reflects a selective fractionation of the BC population, whereby larger and less hydrophobic BC is preferentially scavenged, while a finer pool with higher BC-MAC_{678} becomes relatively more prevalent upon arrival at the distant Indian Ocean receptor observatories. This is consistent with an earlier finding obtained during the winter at the MCOH, where it was observed that BC-MAC_{678} in the rain was lower than BC-MAC_{678} measured for suspended aerosols collected simultaneously from the air (Budhavant et al., 2020). By shedding light on the aging effect of the optical properties of BC aerosols, the study results advance our understanding of this important topic.

These observational constraints in the southern Asian global hotspot region are consistent with global simulation models, which suggest that in ∼ 1–5 d, BC can internally mix with other aerosols (Jacobson et al., 2000). After mixing, the photochemical properties of pure BC are no longer retained due to the coating of other aerosols in the atmosphere, such as sulfates, nitrates, and organics. Observational data on BC MACs in an ambient atmosphere far from immediate sources are rare. Most models use laboratory-based or city-based measurements for MAC and E-MAC values (e.g., Bond and Bergstrom, 2006; Wang et al., 2016). This study can help bridge the gap between model underestimations and observational estimates of BC and absorption aerosol optical depth (AAOD) indicated for southern Asia (Gustafsson and Ramanathan, 2016). These findings can be utilized to refine model estimates of radiative forcing from both BC and BrC for the large-emission region of southern Asia. The severe

air pollution from the IGP spreads over large regional scales across the Indian Ocean. Therefore, understanding the aging effect of the optical and chemical properties of aerosols is important, particularly for this region.

3.5 Light absorption properties of brown carbon

In addition to BC, BrC also affects radiative forcing at ultraviolet wavelengths, although its MAC is an order of magnitude lower than that of BC in the visible wavelength range (Bosch et al., 2014; Kirillova et al., 2013). During the campaign, measurements of WS extracts of BrC show significant differences in light absorption characteristics between the three sampling sites. The average MAC measured at 365 nm (BrC-MAC_{365}) at the BCOB ($1.0 \pm 0.3\,m^2\,g^{-1}$) was 2 to 3 times higher than that measured at the MCOH ($0.3 \pm 0.3\,m^2\,g^{-1}$) and that measured at the MCOG ($0.6 \pm 0.3\,m^2\,g^{-1}$) (Fig. 4). BrC-MAC_{365} measured during this study is broadly within the same range as that measured in earlier studies focusing on fewer locations in the same region (Bikkina and Sarin, 2014; Dasari et al., 2019). Primary BrC emitted from biomass burning appears to be more light-absorptive than secondary aerosols; MAC values obtained at 405 nm ranged from 0.2 to $1.5\,m^2\,g^{-1}$ for humic and fulvic acids and from 0.001 to $0.09\,m^2\,g^{-1}$ for secondary organic aerosols (Lambe et al., 2013), while Chen and Bond (2010) reported a range for primary aerosols of 0.1 to $1.1\,m^2\,g^{-1}$. The average BrC-MAC_{365} value measured during this study was lower than the values reported close to sources in megacities, such as $1.8\,m^2\,g^{-1}$ for Beijing in winter (Cheng et al., 2011), $1.6 \pm 0.5\,m^2\,g^{-1}$ for Delhi (Kirillova et al., 2014), $1.6 \pm 0.1\,m^2\,g^{-1}$ for Kanpur (Choudhary et al., 2018), and $1.5 \pm 0.2\,m^2\,g^{-1}$ for Kathmandu (Chen et al., 2020). This indicates that the BrC MAC decreased by a factor of 3 from the IGP exit to the equatorial Indian Ocean (Fig. 3).

The AAE characterizes the spectral characteristic of BrC. Furthermore, the AAE is often used to characterize BrC from coal combustion, biomass burning, and biofuel burning (Chen and Bond, 2010; Rastogi et al., 2021). The AAE value of BrC is typically reported to be ~ 1 for fossil fuel emissions, ~ 7 for biomass burning, and 7–15 for laboratory-generated smoke and the smoldering of different types of woods (Hoffer et al., 2006; Chen and Bond, 2010). The average AAE values of WS-BrC intercepted at the southern Asian receptor observatories (in the 330–400 nm range) were 5.5 ± 2.7 at the BCOB, 6.5 ± 2.4 at the MCOH, and 4.1 ± 0.5 at the MCOG. These values can be compared with AAE values measured at the Nepal Climate Observatory – Pyramid station (4.9 ± 0.7; Kirillova et al., 2016) and in New Delhi in winter (5.1 ± 2.0; Kirillova et al., 2014). However, the AAE values in this study show differences that are not significant compared to those previously measured at the MCOH in winter (7.2 ± 0.7; Bosch et al., 2014) and at the IGP outflow over the Bay of Bengal (9.1 ± 2.5; Bikkina and Sarin, 2013). The results of this synoptic study, conducted on a large scale across southern Asia, are significant for understanding the aging effect of the optical and chemical properties of aerosols.

3.6 Aerosol radiative forcing

From December to March, the tropical Indian Ocean/atmosphere system provides a natural opportunity to study aerosol radiative forcing influenced by anthropogenic aerosols (Satheesh and Ramanathan, 2000; Nair et al., 2023). This is due to the fact that the Indian Ocean atmosphere receives polluted air that travels from the Indian subcontinent and surrounding regions (Fig. 1; Gustafsson et al., 2009; Budhavant et al., 2018).

Direct aerosol radiative forcing (DARF; cloud-free atmosphere) has been estimated over the BCOB, MCOH, and MCOG on a monthly basis using aerosol optical properties obtained from OPAC in the SBDART model (Fig. 5). The DARF at the top of the atmosphere (TOA; 3 km) and at the surface is calculated by estimating the differences in downward and upward fluxes simulated by the model under atmospheric conditions with and without aerosols for the three sites. The surface forcing and TOA DARF were both negative at all three sampling stations, indicating cooling effects. Meanwhile, the atmospheric column represented a warming effect. The negative sign depicts the dominant presence of scattering aerosols.

This study observed that the average atmospheric forcing at the BCOB was higher ($10.5 \pm 3.2\,W\,m^{-2}$) than that at the MCOG ($4.8 \pm 2.1\,W\,m^{-2}$) and that at the MCOH ($8.0 \pm 2.6\,W\,m^{-2}$). This difference was attributed to anthropogenic aerosols, particularly BC (i.e., net-absorbing BC), which caused a warming effect in the atmosphere (Figs. 2 and 5). The BCOB experienced nearly double the atmospheric forcing compared to the remote equatorial ocean at the MCOG, likely due to its higher concentrations of anthropogenic aerosols, such as BC, NO_3^-, and nss-K^+ (Table S4; Fig. 3). During winter, the IGP experiences a significant increase in aerosol loading, mainly due to carbon aerosols resulting from fossil fuel and biofuel combustion (Gustafsson et al., 2009; Kaskaoutis et al., 2014; Dasari et al., 2020). As spring progresses, dust becomes the dominant aerosol in the northwestern region of India and in arid areas of southwestern Asia (Kaskaoutis et al., 2014; Singh, 2014; Dumka et al., 2023). At the same time, significant agricultural burning in southeastern Asia results in significantly elevated concentrations of carbonaceous aerosols (Kaskaoutis et al., 2014; Budhavant et al., 2015; Bikkina et al., 2019). Additionally, Himalayan forest fires and wheat residue burning in the IGP contribute to the aerosol burden during spring (Gautam et al., 2007; Bikkina et al., 2019). The BCOB experienced high atmospheric forcing in March, particularly in the outflow region of the IGP (Fig. 5). In January, the MCOH experienced slightly higher atmospheric forcing ($11.2\,W\,m^{-2}$) than

the BCOB (10.4 W m^{-2}). These findings are consistent with those of our earlier study conducted at the MCOH, which showed that anthropogenic aerosols, such as BC, nss-K^+, nss-SO_4^{2-}, and NH_4^+, were predominantly in the fine mode (70 %–95 %) and were particularly observed in air masses coming from the IGP during this period (Budhavant et al., 2018). These findings suggest that the outflow region of the IGP is exposed to significant atmospheric-warming effects. Therefore, it is crucial to address this issue and take appropriate measures to reduce the amount of anthropogenic aerosol loading.

4 Summary

The South Asian Pollution Experiment 2018 (SAPOEX-18) utilized access to three strategically located atmospheric receptor observatories to provide synoptic observations of the optical properties of ambient carbonaceous aerosols along the main wintertime flow trajectory from key source regions. The increase in BC-MAC_{678} from the IGP outflow of the BCOB to the receptor stations (MCOH and MCOG) corresponded to about 80 %. Earlier reports for this system have demonstrated that there is no additional enhancement in the BC MAC from aerosol coatings during LRT from the BCOB; this likely reflects a scavenging fractionation, resulting in a population of finer BC with higher MAC_{678} that has a longer lifespan. These observational constraints revealed opposite trends during long-range transport for the BC MAC and BrC MAC, with the BrC MAC decreasing, presumably due to photochemical bleaching. This study also found significant anthropogenic chloride emissions from human activities, which can affect the oxidation capacity of polluted air. Models estimating the climate effects of aerosols, particularly BC aerosols, may have underestimated the ambient BC MAC over distant and extensive receptor areas, potentially contributing to discrepancies in aerosol absorption predicted by models constrained by observations. These findings can be utilized to refine model estimates of radiative forcing from both BC and BrC for the large-emission region of southern Asia. This is particularly relevant as severe air pollution from the Indo-Gangetic Plain spreads over large regional scales across the Indian Ocean.

Data availability. The data supporting this study's findings are available from the corresponding author upon reasonable request.

Supplement. The supplement related to this article is available online at: https://doi.org/10.5194/acp-24-11911-2024-supplement.

Author contributions. KB and ÖG conceived the study. KB collected the samples at the MCOH, AS was responsible for sample collection at the BCOB, and AM was responsible for sample collection at the MCOG. KB performed the chemical analysis with the support of SMG, HRCRN, and MRM; conducted the radiative-forcing estimations; and analyzed the satellite data. KB and ÖG interpreted the data and drafted the paper. All co-authors provided input on the interpretations and early versions of the paper.

Competing interests. The contact author has declared that none of the authors has any competing interests.

Disclaimer. Publisher's note: Copernicus Publications remains neutral with regard to jurisdictional claims made in the text, published maps, institutional affiliations, or any other geographical representation in this paper. While Copernicus Publications makes every effort to include appropriate place names, the final responsibility lies with the authors.

Acknowledgements. Elena Kirillova and Sanjeev Dasari (Stockholm University) are acknowledged for their support during the field campaign. We thank the technical staff at the BCOB, MCOH, and MCOG for their continued field support. Special thanks are due to the Maldives Meteorological Service and the government of the Republic of Maldives for their ongoing support of the joint MCOH–MCOG operation. Krishnakant Budhavant expresses thanks for the additional support from the Regional Resource Centre for Asia and the Pacific (RRC.AP) at the Asian Institute of Technology (AIT), Thailand. We acknowledge financial support from the Swedish Research Council for Sustainable Development (Formas; grant no. 2020-01917) and the Swedish Research Council (VR; grant nos. 2017-01601 and 2020-05384).

Financial support. This research has been supported by the Svenska Forskningsrådet Formas (grant no. 2020-01917) and the Vetenskapsrådet (grant nos. 2017-01601 and 2020-05384).

The publication of this article was funded by the Swedish Research Council, Forte, Formas, and Vinnova.

Review statement. This paper was edited by Manvendra Krishna Dubey and reviewed by two anonymous referees.

References

Ahmed, M., Das, M., Afser, T., Rokonujjaman, M., Akther, T., and Salam, A.: Emission of Carbonaceous Species from Biomass Burning in the Traditional Rural Cooking Stove in Bangladesh, Open J. Air Pollut., 7, 287–297, https://doi.org/10.4236/ojap.2018.74014, 2018.

Andreae, M. O.: Soot carbon and excess fine potassium: long-range transport of combustion-derived aerosols, Science, 220, 1148–1151, https://doi.org/10.1126/science.220.4602.1148, 1983.

Andreae, M. O. and Gelencsér, A.: Black carbon or brown carbon? The nature of light-absorbing carbonaceous aerosols, At-

mos. Chem. Phys., 6, 3131–3148, https://doi.org/10.5194/acp-6-3131-2006, 2006.

Ansari, K. and Ramachandran, S.: Aerosol characteristics over Indo-Gangetic Plain from ground-based AERONET and MERRA-2/CAMS model simulations, Atmos. Environ., 293, 119434, https://doi.org/10.1016/j.atmosenv.2022.119434, 2023.

Bedareva, T. V., Sviridenkov, M. V., and Zhuravleva, T. B.: Retrieval of dust aerosol optical and microphysical properties from ground-based sun-sky radiometer measurements in an approximation of randomly oriental spheroids, J. Quant. Spectrosc. Ra. 146, 140–157, https://doi.org/10.1016/j.jqsrt.2014.05.006, 2014.

Behnke, W. and Zetzsch, C.: Heterogeneous formation of chlorine atoms from various aerosols in the presence of O_3 and HCI, J. Aerosol Sci., 20, 1167–1170, 1989.

Bikkina, S. and Sarin, M. M.: Light absorption organic aerosols (brown carbon) over the tropical Indian Ocean: impact of biomass burning emissions, Environ. Res. Lett., 8, 044042, https://doi.org/10.1088/1748-9326/8/4/044042, 2013.

Bikkina, S. and Sarin, M. M.: $PM_{2.5}$, EC, and OC in the atmospheric outflow from the Indo-Gangetic Plain: Temporal variability and aerosol organic carbon-to-organic mass conversion factor, Sci. Total Environ., 487, 196–205, https://doi.org/10.1016/j.scitotenv.2014.04.002, 2014.

Bikkina, S., Andersson, A., Kirillova, E. N., Holmstrand, H., Tiwari, S., Srivastava, A. K., Bisht, D. S., and Gustafsson, Ö.: Air quality in megacity Delhi affected by countryside biomass burning, Nat. Sustain., 2, 200–205, https://doi.org/10.1038/s41893-019-0219-0, 2019.

Birch, M. E. and Cary, R. A.: Elemental Carbon-Based Method for Monitoring Occupational Exposures to Particulate Diesel Exhaust, Aerosol Sci. Tech., 25, 221–241, https://doi.org/10.1080/02786829608965393, 1996.

Bollasina, M. A., Ming, Y., and Ramaswamy, V.: Anthropogenic Aerosols and the Weakening of the South Asian Summer Monsoon, Science, 334, 502–505, https://doi.org/10.1126/science.1204994, 2011.

Bond, T. C. and Bergstrom, R. W.: Light absorption by carbonaceous particles: An investigative review, Aerosol Sci. Tech., 40, 27–67, https://doi.org/10.1080/02786820500421521, 2006.

Bosch, C., Andersson, A., Kirillova, E. N., Budhavant, K., Tiwari, S., Praveen, P. S., Russell, L. M., Beres, N. D., Ramanathan, V., and Gustafsson, Ö.: Source-diagnostic dual-isotope composition and optical properties of water-soluble organic carbon and elemental carbon in the South Asian outflow intercepted over the Indian Ocean. J. Geophys. Res.-Atmos., 119, 11743–11759, https://doi.org/10.1002/2014JD022127, 2014.

Brimblecombe, P. and Clegg, S.: The solubility and behavior of acid gases in the marine aerosol, J. Atmos. Chem., 7, 1–18, 1988.

Budhavant, K., Andersson, A., Bosch, C., Krusa, M., Kirillova, E. N., Sheesley, R. J., Safai, P. D., Rao, P. S. P., Gustafsson, Ö.: Radiocarbon-based source apportionment of elemental carbon aerosols at two South Asian receptor observatories over a full annual cycle, Environ. Res. Lett., 10, 064004, https://doi.org/10.1088/1748-9326/10/6/064004, 2015.

Budhavant, K., Andersson, A., Holmstrand, H., Bikkina, P., Bikkina, S., Satheesh, S. K., and Gustafsson, Ö.: Enhanced Light-Absorption of Black Carbon in Rainwater Compared with Aerosols Over the Northern Indian Ocean, J. Geophys. Res., 125, e2019JD031246, https://doi.org/10.1029/2019JD031246, 2020.

Budhavant, K., Andersson, A., Holmstrand, H., Satheesh, S. K., and Gustafsson, Ö.: Black carbon aerosols over Indian Ocean have unique source fingerprints and optical characteristics during monsoon season, P. Natl. Acad. Sci. USA, 120, e2210005120, https://doi.org/10.1073/pnas.2210005120, 2023.

Budhavant, K., Bikkina, S., Andersson, A., Asmi, E., Kesti, J., Zahid, H., Satheesh, S. K., and Gustafsson Ö.: Anthropogenic fine aerosols dominate the wintertime regime over the northern Indian Ocean, Tellus B, 70, 1464871, https://doi.org/10.1080/16000889.2018.1464871, 2018.

Chakrabarty, R. K., Gyawali, M., Yatavelli, R. L. N., Pandey, A., Watts, A. C., Knue, J., Chen, L.-W. A., Pattison, R. R., Tsibart, A., Samburova, V., and Moosmüller, H.: Brown carbon aerosols from burning of boreal peatlands: microphysical properties, emission factors, and implications for direct radiative forcing, Atmos. Chem. Phys., 16, 3033–3040, https://doi.org/10.5194/acp-16-3033-2016, 2016.

Chen, Y. and Bond, T. C.: Light absorption by organic carbon from wood combustion, Atmos. Chem. Phys., 10, 1773–1787, https://doi.org/10.5194/acp-10-1773-2010, 2010.

Chen, P., Kang, K., Tripathee, L., Ram, K., Rupakheti, M., Panday, A. K., Zhang, Q., Guo, J., Wang, X., Pu, T., and Li, C.: Light absorption properties of elemental carbon (EC) and water-soluble brown carbon (WS-BrC) in the Kathmandu Valley, Nepal: a 5-year study, Environ. Pollut., 261, 114239, https://doi.org/10.1016/j.envpol.2020.114239, 2020.

Cheng, Y., He, K.-B., Zheng, M., Duan, F.-K., Du, Z.-Y., Ma, Y.-L., Tan, J.-H., Yang, F.-M., Liu, J.-M., Zhang, X.-L., Weber, R. J., Bergin, M. H., and Russell, A. G.: Mass absorption efficiency of elemental carbon and water-soluble organic carbon in Beijing, China, Atmos. Chem. Phys., 11, 11497–11510, https://doi.org/10.5194/acp-11-11497-2011, 2011.

Cheng, Y., He, K., Du, Z., Engling, G., Liu, J., Ma, Y., Zheng, M., and Weber, R. J.: The characteristics of brown carbon aerosol during winter in Beijing, Atmos. Environ., 127, 355–364, https://doi.org/10.1016/j.atmosenv.2015.12.035, 2016.

Choudhary, V., Rajput, P., Singh, D. K., Singh, A. K., and Gupta, T.: Light absorption characteristics of brown carbon during foggy and non-foggy episodes over the Indo-Gangetic Plain, Atmos. Pollut. Res. 9, 494–501, https://doi.org/10.1016/j.apr.2017.11.012, 2018.

Corbett, J. J. and Koehler, H. W.: Updated emissions from ocean shipping, J. Geophys. Res.-Atmos., 108, 4650, https://doi.org/10.1029/2003JD003751, 2003.

Corrigan, C. E., Ramanathan V., and Schauer, J. J.: Impact of monsoon transition on the physical and optical properties of aerosols, J. Geophys. Res., 111, D18208, https://doi.org/10.1029/2005JD006370, 2006.

Dasari, S., Andersson, A., Bikkina, S., Holmstrand, H., Budhavant, K., Satheesh, S., Backman, J., Kesti, J., Asmi, E., Salam, A., Bisht, D. S., Tiwari, S., Zahid, A., and Gustafsson, Ö.: Photochemical degradation affects the light absorption of water-soluble brown carbon in the South Asian outflow, Sci. Adv., 5, eaau8066, https://doi.org/10.1126/sciadv.aau8066, 2019.

Dasari, S., Andersson, A., Stohl, A., Evangeliou, N., Bikkina, S., Holmstrand, H., Budhavant, K., Salam, A., and Gustafsson, Ö.: Source quantification of South Asian black carbon aerosols with isotopes and modelling, Environ. Sci. Technol. 54, 11771–11779, https://doi.org/10.1021/acs.est.0c02193, 2020.

Draxler, R. R.: HYSPLIT4 user's guide, NOAA Tech. Memo. ERL ARL-230, NOAA Air Resources Laboratory, Silver Spring, MD, https://arl.noaa.gov/wp_arl/wp-content/uploads/documents/reports/arl-230.pdf (last access: 16 October 2024), 1999.

Draxler, R. R. and Hess, G. D.: Description of the HYSPLIT_4 modeling system, NOAA Tech. Memo. ERL ARL-224, NOAA Air Resources Laboratory, Silver Spring, MD, 24 pp., https://arl.noaa.gov/wp_arl/wp-content/uploads/documents/reports/arl-230.pdf (last access: 16 October 2024), 1997.

Dumka, U. C., Kosmopoulos, P., Baxevanaki, E., Kaskaoutis, D. G., Huda, M. N., Khan, F., Bilal, M., Ambade, B., Khanal, S., and Munshi, P.: Surface Radiative forcing as a Climate-Change Indicator in North India due to the Combined effects of Dust and Biomass Burning, Fire, 6, 365, https://doi.org/10.3390/fire6090365, 2023.

Gautam, R., Hsu, N. C., Kafatos, M., and Tsay, S. C.: Influences of winter haze on fog/low cloud over the Indo-Gangetic plains, J. Geophys. Res., 112, D05207, https://doi.org/10.1029/2005JD007036, 2007.

Gopikrishnan, G. S. and Kuttippurath, J.: A decade of satellite observations revealed a significant increase in atmospheric formaldehyde from shipping in the Indian Ocean, Atmos. Environ., 246, 118095, https://doi.org/10.1016/j.atmosenv.2020.118095, 2021.

Granat, L., Engström, J. E., Praveen, S., and Rodhe, H.: Light absorbing material (soot) in rainwater and in aerosol particles in the Maldives, J. Geophys. Res., 115, 1–12, https://doi.org/10.1029/2009JD013768, 2010.

Gustafsson, Ö. and Ramanathan, V.: Convergence on climate warming by black carbon aerosols, P. Natl Acad. Sci. USA, 113, 4243–4245, https://doi.org/10.1073/pnas.1603570113, 2016.

Gustafsson, O., Krusa, M., Zencak, Z., Sheesley, R. J., Granat, L., Engstrom, E., Praveen, P. S., Leck, C., and Rodhe, H.: Brown Clouds over South Asia: Biomass or Fossil Fuel Combustion?, Science, 323, 495–498, https://doi.org/10.1126/science.1164857, 2009.

Guttikunda, S. K. and Jawahar, P.: Atmospheric emissions and pollution from the coal-fired thermal power plants in India, Atmos. Environ., 92, 449–460, https://doi.org/10.1016/j.atmosenv.2014.04.057, 2014.

Haslett, S. L., Bell, D. M., Kumar, V., Slowik, J. G., Wang, D. S., Mishra, S., Rastogi, N., Singh, A., Ganguly, D., Thornton, J., Zheng, F., Li, Y., Nie, W., Liu, Y., Ma, W., Yan, C., Kulmala, M., Daellenbach, K. R., Hadden, D., Baltensperger, U., Prevot, A. S. H., Tripathi, S. N., and Mohr, C.: Nighttime NO emissions strongly suppress chlorine and nitrate radical formation during the winter in Delhi, Atmos. Chem. Phys., 23, 9023–9036, https://doi.org/10.5194/acp-23-9023-2023, 2023.

Hess, M., Koepke, P., and Schult, I.: Optical properties of aerosols and clouds: The software package OPAC, B. Am. Meteorol. Soc., 79, 831–844, https://doi.org/10.1175/1520-0477(1998)079<0831:OPOAAC>2.0.CO;2, 1998.

Hoffer, A., Gelencsér, A., Guyon, P., Kiss, G., Schmid, O., Frank, G. P., Artaxo, P., and Andreae, M. O.: Optical properties of humic-like substances (HULIS) in biomass-burning aerosols, Atmos. Chem. Phys., 6, 3563–3570, https://doi.org/10.5194/acp-6-3563-2006, 2006.

Holben, B. N., Eck, T. F., Slutsker, I., and Smirnov, A.: AERONET – a federal instrument network and data archive for aerosol characterization, Remote Sens. Environ., 66, 1–16, 1998.

Höpner, F., Bender, F. A.-M., Ekman, A. M. L., Praveen, P. S., Bosch, C., Ogren, J. A., Andersson, A., Gustafsson, Ö., and Ramanathan, V.: Vertical profiles of optical and microphysical particle properties above the northern Indian Ocean during CARDEX 2012, Atmos. Chem. Phys., 16, 1045–1064, https://doi.org/10.5194/acp-16-1045-2016, 2016.

IPCC: Climate Change 2013: The Physical Science Basis, Summary for Policymakers. Contribution of Working Group I to the Fifth Assessment Report of the Intergovernmental Panel on Climate Change, edited by: Stocker, T. F., Qin, D., Plattner, G. K., Tignor, M., Allen, S. K., Boschung, J., Nauels, A., Xia, Y., Bex, V., and Midgley, P. M., Cambridge University Press, Cambridge, United Kingdom and New York, NY, USA, https://doi.org/10.1017/CBO9781107415324, 2013.

Jacobson, M. C., Hansson, H. C., Noone, K. J., and Charlson, R. J.: Organic atmospheric aerosols: review and state of the science, Rev. Geophys., 38, 267–294, https://doi.org/10.1029/1998RG000045, 2000.

Kaskaoutis, D. G., Kumar, S., Sharma, D., Singh, R. P., Kharol, S. K., Sharma, M., Singh, K., Singh, S., Singh, A., and Singh, D.: Effects of crop residue burning on aerosol properties, plume characteristics, and long-range transport over northern India, J. Geophys. Res., 119, 5424–5444, https://doi.org/10.1002/2013JD021357, 2014.

Keene, W. C., Pszenny, A. P., Galloway, J. N., and Hawley, M. E.: Sea-salt corrections and interpretation of constituent ratios in marine precipitation, J. Geophys. Res.-Atmos., 91, 6647, https://doi.org/10.1029/JD091iD06p06647, 1986.

Kirillova, E. N., Sheesley, R. J., Andersson, A., and Gustafsson, Ö.: Natural abundance ^{13}C and ^{14}C analysis of water-soluble organic carbon (WSOC) in atmospheric aerosols, Anal. Chem., 82, 7973–7978, https://doi.org/10.1021/ac1014436, 2010.

Kirillova, E. N., Andersson, A., Sheesley, R. J., Kruså, M., Praveen, P. S., Budhavant, K., Safai, P. D., Rao, P. S. P., and Gustafsson, Ö.: ^{13}C- and ^{14}C-based study of sources and atmospheric processing of water-soluble organic carbon (WSOC) in South Asian aerosols, J. Geophys. Res.-Atmos., 118, 614–626, https://doi.org/10.1002/jgrd.50130, 2013.

Kirillova, E. N., Andersson, A., Tiwari, S., Kumar Srivastava, A., Singh Bisht, D., and Gustafsson, Ö.: Water-soluble organic carbon aerosols during a full New Delhi winter: Isotope-base source apportionment and optical properties, J. Geophys. Res.-Atmos., 119, 3476–3485, https://doi.org/10.1002/2013JD020041, 2014.

Kirillova, E. N., Marinoni, A., Bonasoni, P., Vuillermoz, E., Faccchini, M. C., Fuzzi, S., and Decesari, S.: Light absorption properties of brown carbon in the high Himalayas, J. Geophys. Res.-Atmos., 121, 9621–9639, https://doi.org/10.1016/j.envpol.2020.114239, 2016.

Kuttippurath, J., Patel, V. K., Pathak, M., and Singh, A.: Improvements in SO_2 pollution in India: role of technology and environmental regulations, Environ. Sci. Pollut. R., 29, 78637–78649, https://doi.org/10.1007/s11356-022-21319-2, 2022.

Lambe, A. T., Cappa, C. D., Massoli, P., Onasch, T. B., Forestieri, S. D., Martin, A. T., Cummings, M. J., Croasdale, D. R., Brune, W. H., Worsnop, D. R., and Davidovits, P.: Relationship between oxidation level and optical properties of sec-

ondary organic aerosols, Environ. Sci. Technol., 47, 6349–6357, https://doi.org/10.1021/es401043j, 2013.

Laskin, A., Laskin, J., and Nizkorodov, S. A.: Chemistry of atmospheric brown carbon, Chem. Rev., 115, 4335–4382, https://doi.org/10.1021/cr5006167, 2015.

Lelieveld, J., Evans, J. S., Fnais, M., Giannadaki, D., and Pozzer, A.: The contribution of outdoor air pollution sources to premature mortality on a global scale, Nature, 525, 367–371, https://doi.org/10.1038/nature15371, 2015.

Lin, Y., Wang, Y., Hsieh, J.-S., Jiang, J. H., Su, Q., Zhao, L., Lavallee, M., and Zhang, R.: Assessing the destructiveness of tropical cyclones induced by anthropogenic aerosols in an atmosphere–ocean coupled framework, Atmos. Chem. Phys., 23, 13835–13852, https://doi.org/10.5194/acp-23-13835-2023, 2023.

Liu, J., Bergin, M., Guo, H., King, L., Kotra, N., Edgerton, E., and Weber, R. J.: Size-resolved measurements of brown carbon in water and methanol extracts and estimates of their contribution to ambient fine-particle light absorption, Atmos. Chem. Phys., 13, 12389–12404, https://doi.org/10.5194/acp-13-12389-2013, 2013.

Lu, F., Chen, S., Hu, Z., Han, Z., Alam, K., Luo, H., Bi, H., Chen, J., and Guo, X.: Sensitivity and uncertainties assessment in radiative forcing due to aerosol optical properties in diverse locations in China, Sci. Total Environ., 860, 160447, https://doi.org/10.1016/j.scitotenv.2022.160447, 2023.

Mauderly, J. L. and Chow, J. C.: Health effects of organic aerosols, Inhal. Toxicol., 20, 257–288, https://doi.org/10.1080/08958370701866008, 2008.

Nair, H., Budhavant, K., Manoj, M. R., Andersson, A., Satheesh, S. K., Ramanathan, V., and Gustafsson, Ö.: Aerosol demasking enhances climate warming over South Asia, NPJ Clim. Atmos. Sci., 6, 39, https://doi.org/10.1038/s41612-023-00367-6, 2023.

Nair, H. R. C. R., Budhavant, K., Manoj, M. R., Kirillova, E. N., Satheesh, S. K., and Gustafsson, Ö.: Roles of water-soluble aerosol coatings for the enhanced radiative absorption of black carbon over south asia and the northern indian ocean, Sci Tot. Environ., 926, 171721, https://doi.org/10.1016/j.scitotenv.2024.171721, 2024.

Orsini, C. Q., Tabacniks, M. H., Artaxo, P., Andrade, M. F., and Kerr, A. S.: Characteristics of fine and coarse particles of natural and urban aerosols of Brazil, Atmos. Environ., 20, 2259–2269, https://doi.org/10.1016/0004-6981(86)90316-1, 1986.

Paris, R., Desboeufs, K. V., Formenti, P., Nava, S., and Chou, C.: Chemical characterisation of iron in dust and biomass burning aerosols during AMMA-SOP0/DABEX: implication for iron solubility, Atmos. Chem. Phys., 10, 4273–4282, https://doi.org/10.5194/acp-10-4273-2010, 2010.

Pathak, G., Nichter, M., Hardon, A., Moyer, E., Latkar A., Simbaya, J., Pakasi, D., Taqueban, E., and Love, J.: Plastic pollution and the open burning of plastic wastes, Global Environ. Change, 80, 102648, https://doi.org/10.1016/j.gloenvcha.2023.102648, 2023.

Ram, K. and Sarin, M. M.: Absorption coefficient and site-specific mass absorption efficiency of elemental carbon in aerosols over Urban, Rural, and high-altitude sites in India, Environ. Sci. Technol., 43, 8233–8239, https://doi.org/10.1021/es9011542, 2009.

Ramachandran, S., Rupakheti, M., Cherian, R., and Lawrence, M. G.: Aerosols heat up the Himalayan climate, Sci. Total Environ., 894, 164733, https://doi.org/10.1016/j.scitotenv.2023.164733, 2023.

Ramanathan, V. and Carmichael, G.: Global and regional climate changes due to black carbon, Nat. Geosci., 1, 221–227, https://doi.org/10.1038/ngeo156, 2008.

Ramanathan, V., Chung, C., Kim, D., Bettge, T., Kiehl, J. T., Washington, W. M., Fu, Q., Sikka, D. R., and Wild, M.: Atmospheric brown clouds: Impacts on South Asian climate and hydrological cycle, P. Natl. Acad. Sci. USA, 102, 5326–5333, https://doi.org/10.1073/pnas.0500656102, 2005.

Ramanathan, V., Ramana, M. V., Roberts, G., Kim, D., Corrigan, C., Chung, C., and Winker, D.: Warming trends in Asia amplified by brown cloud solar absorption, Nature, 448, 575–578, https://https://doi.org/10.1038/nature06019, 2007.

Rastogi, N., Satish, R., Singh, A., Kumar, V., Thamban, N., Lalchandani, V., Shukla, A., Vats, P., Tripathi, S. N., and Ganguly, D.: Diurnal variability in the spectral characteristic and sources of water-soluble brown carbon aerosols over Delhi, Sci. Total Environ., 794, 148589, https://doi.org/10.1016/j.scitotenv.2021.148589, 2021.

Ricchiazzi, P., Yang, S., Gautier, C., and Sowle, D.: SBDART: A research and teaching tool for plane-parallel radiative transfer in the earth's atmosphere, B. Am. Meteorol. Soc., 79, 2101–2114, https://doi.org/10.1175/1520-0477(1998)079<2101:SARATS>2.0.CO;2, 1998.

Ruellan, S. and Cachier, H.: Characterization of fresh particulate vehicular exhausts near a Paris high flow road, Atmos. Environ., 35, 453–468, https://doi.org/10.1016/S1352-2310(00)00110-2, 2001.

Satheesh, S. K.: Radiative forcing by aerosols over Bay of Bengal region, Geophys. Res. Lett., 29, 2083, https://doi.org/10.1029/2002GL015334, 2002.

Satheesh, S. K. and Ramanathan, V.: Large difference in tropical aerosol forcing at the top of the atmosphere and Earth's surface, Nature, 405, 60–63, https://doi.org/10.1038/35011039, 2000.

Shindell, D., Kulenstierna, J. C., Vignati, E., Dingenen, R. V., Amann, M., Klimount, Z., Anenberg, S. C., Mulller, N., Jansessens-Maenhout, G., Raes, F., and Schwartz, J.: Simultaneously Mitigating Near-Term Climate Change and Improving Human Health and Food Security, Science, 335, 183–189, https://doi.org/10.1126/science.1210026, 2012.

Shohel, M., Kistler, M., Rahman, M. A., Kasper-Giebl, A., Reid, J. S., and Salam A.: Chemical characterization of $PM_{2.5}$ collected from a rural coastal island of the Bay of Bengal (Bhola, Bangladesh), Environ. Sci. Pollut. R., 25, 4558–4569, https://doi.org/10.1007/s11356-017-0695-6, 2018.

Singh, R. P.: Dust storms and their influence on atmospheric parameters over the Indo-Gangetic plains, 21–35, chap. 2, in: Geospatial technologies and climate change, edited by: Sundaresan, J., Santosh, K., Déri, A., Roggema, R., and Singh, R., 10, https://doi.org/10.1007/978-3-319-01689-4_2, 2014.

Stamnes, K., Tsay, S. C., Wiscombe, W., and Jayaweera, K.: Numerically stable algorithm for discrete ordinate-method radiative transfer in multiple scattering and emitting layered media, Appl. Optics, 27, 2502–2509, https://doi.org/10.1364/AO.27.002502, 1988.

Stone, E. A., Lough, G. C., Schauer, J. J., Praveen, P. S., Corrigan, C. E., and Ramanathan, V.: Understanding the origin of black carbon in the atmospheric brown cloud

over the Indian Ocean, J. Geophys. Res., 122, D22S23, https://doi.org/10.1029/2006JD008118, 2007.

Venkataraman, C., Bhushan, M., Dey, Ganguly, S. D., Gupta, T., Habib, G., Kesarkar, A., Phuleria, H., and Sunder Raman, R.: Indian Network Project on Carbonaceous Aerosol Emissions, Source Apportionment and Climate Impacts (COALESCE), B. Am. Meteorol. Soc., E1052–E1068, https://doi.org/10.1175/BAMS-D-19-0030.1, 2020.

Vogt, R., Crutzen, P. J., and Sander, R.: A mechanism for halogen release from sea-salt aerosol in the remote marine boundary layer, Nature, 383, 327–330, 1996.

Wang, X., Heald, C. L., Sedlacek, A. J., de Sá, S. S., Martin, S. T., Alexander, M. L., Watson, T. B., Aiken, A. C., Springston, S. R., and Artaxo, P.: Deriving brown carbon from multiwavelength absorption measurements: method and application to AERONET and Aethalometer observations, Atmos. Chem. Phys., 16, 12733–12752, https://doi.org/10.5194/acp-16-12733-2016, 2016.

Weingartner, E., Saathoff, H., Schnaiter, M., Streit, N., Bitnar, B., and Baltensperger, U.: Absorption of light by soot particles: Determination of the absorption coefficient using Aethalometers, J. Aerosol. Sci., 34, 1445–1463, https://doi.org/10.1016/S0021-8502(03)00359-8, 2003.

WHO: Country Estimates on Air Pollution Exposure and Health Impact, World Health Organisation, http://www.who.int/mediacentre/news/releases/2016/air-pollution-estimates/en/ (last access: 20 October 2024), 2016.